I-V-T and DLTS characteristics of e-beam deposited W/Pd Schottky contacts on 4H-SiC

A T Paradzah, M J Legodi, F D Auret, M W Diale and W E Meyer

Department of Physics, University of Pretoria, Private Bag X20, Hatfield 0028 Pretoria

Alexander.Paradzah@up.ac.za

Abstract. We report on the characteristics of W/Pd Schottky contacts deposited on 4H-SiC. I-V-T measurements indicate a deviation from thermionic emission (*TE*) theory in the 40 K to 100 K temperature range, suggesting an inhomogeneous Schottky barrier at the interface. This observed deviation could be due to the surface damage caused by e-beam deposition. Both the Schottky barrier height (Φ_{BO}) and the diode ideality factor (n) exhibited anomalous behaviour in the low doped (7.1×10^{15} cm^{-3}) and highly doped (1.96×10^{16} cm^{-3}) samples. In the 1.96×10^{16} cm^{-3} doped sample, we typically observed $1.50\ eV \leq \Phi_{BO} \leq 0.89\ eV$ and $1.1 \leq n \leq 4.3$ in the temperature range 340 K to 40 K. The inhomogeneous Schottky barrier was satisfactorily described by a Gaussian distribution with mean, $\Phi_{BO} = 1.73$ eV, and standard deviation, $\sigma_s = 0.09$ eV. Deep level transient spectroscopy (DLTS) reveals the presence of two prominent peaks located at 0.096 eV and 0.607 eV below the conduction band minima, E_C. We detect, on the sample with a doping density of 7.1×10^{15} cm^{-3} (but not on the higher doped sample), two extra peaks with activation enthalpies of 0.160 eV and 0.121 eV which, we attribute to the e-beam metallization damage.

1. Introduction

The wide bandgap, high-thermal conductivity, high-breakdown field, and robust mechanical properties of SiC make it an attractive material for high- temperature, high-power, and high-frequency electronic devices [1-2]. The 4H polytype of SiC has generated much interest recently because of its outstanding electronic properties. It is a promising semiconductor for ionizing radiation detectors as well as for devices that operate in high temperatures and harsh radiation fields due to its wide bandgap [3-4]. Despite the material's high quality physical and electronic properties, SiC devices critically depend on the quality of the metal contacts formed, for example, Schottky contacts i.e., the types of metals used and fabrication factors such as surface cleaning and metallization processes. The quality of a Schottky diode is directly related to the barrier height. A high Schottky barrier height limits the amount of current as fewer charge carriers will have sufficient energy to overcome the barrier and a small barrier height can lead to large amounts of undesired leakage currents. In this work we investigate the behavior of a tungsten contact on n-type 4H-SiC. According to the Schottky-Mott theory, the Schottky barrier height (Φ_{BO}) is defined as $\Phi_{BO} = \Phi_m - \chi$ [5] where Φ_m is the metal work function and χ is

the semiconductor electron affinity. χ = 3.3 eV for SiC and Φ_m = 4.55 eV for tungsten, then the theoretical barrier height is 1.25 eV. However, SBH's of practical Schottky diodes are complicated affairs as they also depend on other factors such as the surface morphology of the underlying semiconductor, its doping density, the details of the metal-semiconductor (MS) interface and the metallization process. The theoretical value is therefore difficult to achieve in practice. The metallization process can also introduce electrically active defects in a material. Knowledge of these defects is vital because electrically active defects can either enhance or degrade device performance by altering the doping concentrations and carrier lifetimes [6-7]. It is thus important to identify, understand and possibly control these defects to enhance device operation [6-8]. In this study we use I-V-T methods to determine the Schottky barrier height and ideality factors of W/Pd contacts on SiC samples of different doping densities. This gives us insight into the nature of Schottky junction formed and its characteristics over a wide temperature range. From DLTS, we describe the electrically active defects that are associated with the metallization damage.

2. Experimental procedure

Samples of n-4H-SiC with doping densities 7.1×10^{15} cm^{-3} and 1.96×10^{16} cm^{-3} were degreased by boiling in trichloroethylene followed by a boil in isopropyl alcohol and rinses in 18 MΩ cm de-ionized water. The native oxide layer on the samples was removed by dipping them in 40% HF solution before a final rinse in de-ionized water and a blow dry in N_2. Low resistance Ni ohmic contacts were deposited on the sample backsides by joule evaporation. The ohmic contacts are 300 nm thick and were annealed in a tube furnace, in flowing Argon gas at 950 °C for 10 minutes. The samples were then rinsed in deionised water and dipped in HF before W/Pd Schottky contacts with relative thickness of 15 nm and 35 nm, and 0.6 mm diameter were e-beam deposited through a metal contact mask. Current-voltage-temperature measurements in the temperature range 20 K to 380 K were carried out in a Helium cryostat. DLTS measurements were performed using a Laplace-DLTS National Instruments DAQ system.

3. Results and discussion

Unless or otherwise stated, all the experimental data are from the 7.1×10^{15} cm^{-3} specimens. Figure 1 shows the semi-logarithmic forward current-voltage characteristics of a typical 7.1×10^{15} cm^{-3} doped sample. The high temperature curves are linear over many orders of magnitude indicating the dominance of the *TE* mechanism. The curves below 140 K show two distinct linear regions. The low voltage "knees" are possibly due to the effect of recombination-generation of carriers in the space charge region and defect-assisted tunneling of charges through the barrier [9]. The curves corresponding to temperatures higher than 140 K are linear – in agreement with the *TE* theory.

According to the *TE* theory, the total majority carrier current, *I*, through a Schottky barrier diode (SBD) may be expressed as [9-10] $I = I_O \exp\left(q\left(V - IR_S\right)/nkT\right)\left[1-\exp\left(q\left(V - IR_S\right)/kT\right)\right]$, where $I_O = AA^*\exp\left(-q\Phi_{BO}/kT\right)$ is the saturation current, q is the electronic charge, A^* the effective Richardson constant, A the effective diode area, T the absolute temperature, Φ_{BO} the zero bias barrier height, k the Boltzmann constant, V the bias voltage, n the ideality factor and R_s the series resistance. An ideality factor, n is introduced to describe the deviation of the experimental I - V results from the ideal *TE* model and is given by: $n = \left(q/kT\right)\left(dV/d\ln I\right)^{-1}$. The linear part of the curves of Figure (1) thus gives the values of n from the gradient. Figure 2 shows variation of experimental n and Φ_{BO} with temperature.

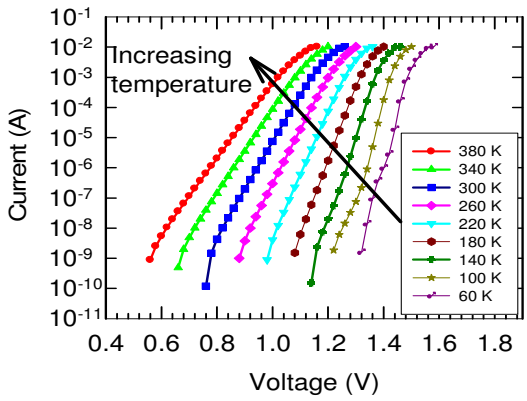

Figure 1. Selected forward *I-V* characteristics in the 60 K – 340 K range for the 7.1×10^{15} cn^{-3} sample.

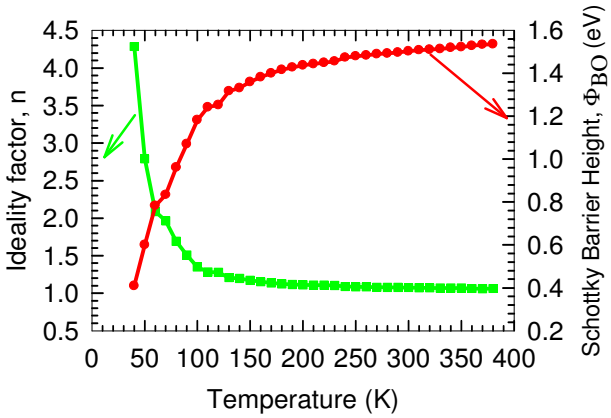

Figure 2. Dependency of barrier height and ideality factor on temperature in the range 40K – 380K

The ideality factor decreases from 4.3 at 40 K to 1.1 at 380 K while Φ_{BO} increases from 0.89 eV at 40 K to 1.50 eV at 380 K. The graph shows that both n and Φ_{BO} have a strong reciprocal dependence on temperature for lower temperatures. This dependency is clearly in two distinct temperature regions where the change in n and Φ_{BO} is more pronounced for $T < 140$ K and less so for $T > 140$ K. For the 1.96×10^{16} cm^{-3} specimen, n decreases from 4.68 at 40 K to 1.09 at 340 K while Φ_{BO} increases from 0.253 eV to 1.42 eV in the same temperature range. Table 1 shows the changes in n and Φ_{BO} with temperature for the two differently doped samples. Since the only variable in the two samples is the doping density, it can be concluded that at any given temperature, Φ_{BO} decreases while n increases with increasing doping density which is in agreement with results of previous studies [11-12]. One can also conclude that lowly doped samples produce better quality SBD characteristics.

Table 1. Variation of n and Φ_{BO} with temperature for selected temperature values.

	$N_D = 7.1\times10^{15}$ cm^{-3}		$N_D = 1.96\times10^{16}$ cm^{-3}	
T (K)	n	Φ_{B0} (eV)	n	Φ_{B0} (eV)
40	4.29	0.41	4.68	0.36
50	2.79	0.60	3.63	0.46
60	2.09	0.78	2.92	0.57
300	1.08	1.50	1.09	1.44

3.1. The Richardson constant

The Richardson plot is used to determine the effective barrier height and the Richardson constant. A plot of ln (I_o / T^2) versus $(1 / T)$ should give a straight line with a slope corresponding to $q\Phi_{BO}/k$ and the intercept should give $ln\ AA^*$. From the Richardson plot, Figure 4(b), A^* has been calculated as 13.2×10^{-3} A cm^{-2} K^{-2} a value that is way too smaller than the expected value of 149 A cm^{-2} K^{-2}. The effective barrier height was calculated to be 0.59 eV. The deviation of the value of A^* from the theoretical value cannot be explained by the thermionic emission diffusion (*TED*) model [12]. Instead, the existence of barrier fluctuations at the interface between the *MS* interface is suggested as the possible cause of the anomalies [13]. Other possible causes of the deviations include existence of crystal defects, image force lowering, effects of tunneling current through the potential barrier, non-uniformity in the interfacial charges, and spatial distribution of the doping atoms [12,14-15].

3.2 Barrier height inhomogeneity analysis and the modified Richardson plot

If a Gaussian distribution of SBH's is assumed, a plot of $\Phi_{ap} vs. 1/2kT$, Figure 4 (a) should give a straight line whose intercept corresponds to Φ_{BO} while its gradient gives σ_{so}^2.

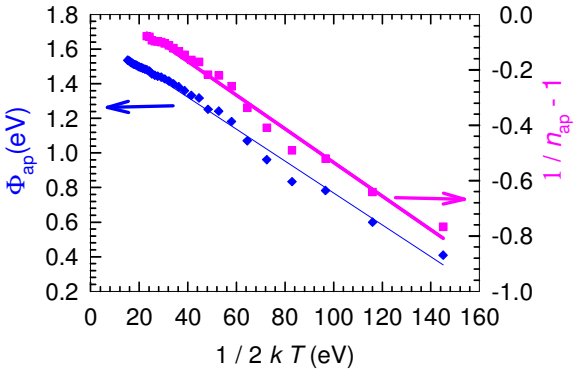

Figure 4 (a). Graph of $1/n_{ap}$ -1 and Φ_{ap} vs. 1/2kT for the determination of ρ_2, ρ_3, and σ_{so}

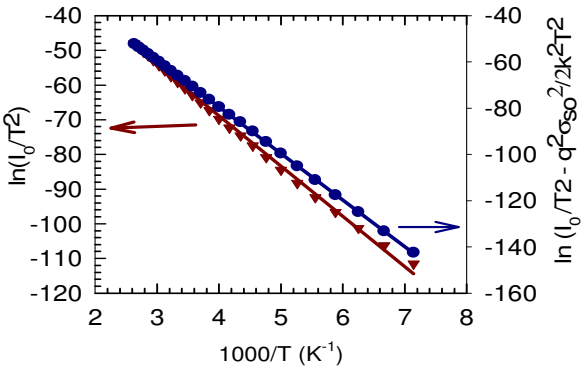

Figure 4 (b). The Richardson plot of and the modified Richardson plot

Values of 0.56 eV and 0.09 eV are obtained from the plot for Φ_{BO} and σ_{so} respectively. Figure 4(a) also shows a plot of $1/n_{ap} - 1$ vs. $1/2kT$ which yields a straight line with an intercept that corresponds to ρ_2 while the gradient gives ρ_3. ρ_2 is found to be -0.53 and ρ_3 is -0.006. The straight line nature of the plot confirms that the ideality in the *I-V* curves represents the voltage deformation of the barrier height at the MS interface [16]. σ_{so} is used to modify the conventional Richardson plot which is constructed from $\ln\left(I_0/T^2\right) - q^2\sigma_{so}^2/2k^2T^2 = \ln AA^* - q\Phi_{BO}/kT$ through a plot of $\ln I_0/T^2 - q^2\sigma_{so}^2/2k^2T^2$ vs. $1/T$.

Figure 4(b) gives an intercept equivalent to $lnAA^*$ and a gradient corresponding to Φ_{BO}. A^* is found to be 25.5Acm^{-2}K^{-2} and Φ_{BO} is obtained as1.734 eV. The value of A^* obtained from Figure 4(b) is still not close to the theoretical value. The reason is likely that a more complicated distribution is needed, say a double Gaussian, as can be seen by the clearly non linearity of Figure 4(a).

3.3 DLTS analysis of e-beam induced defects.

Figure 5(a) shows the DLTS spectrum of the 7.1×10^{15} cm^{-3} doped material after e-beam deposition. The spectrum reveals the presence of two prominent peaks at 0.09 eV and 0.67 eV. These two defects were also observed in the same SiC material albeit with resistively evaporated nickel Schottky contacts. The resistive evaporation would have imparted very minimal lattice damage to the SiC, unlike e0beam metallization. The shallower defect is the nitrogen donor and the deeper level is the Z1/Z2 defect complex. Two additional peaks at 0.12 eV and 0.16 eV are also observed.

Figure 5(b) is the Arrhenius plot of log T^2/e vs. $1000/T$. It shows the levels detected by DLTS measurements recorded at a quiescent reverse bias of -1 V, a forward filling pulse of 0.2 V and a rate window of 1000 s^{-1}.

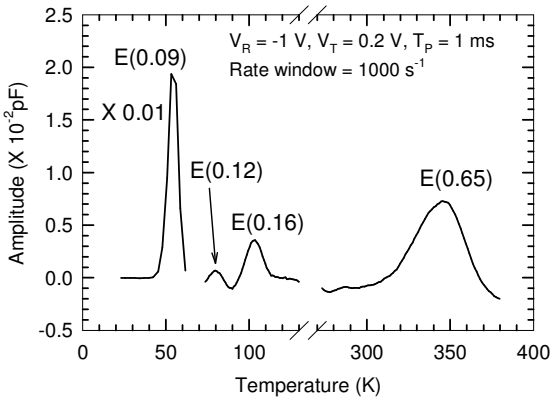

Figure 5 (a). DLTS Spectra obtained at 1000 s^{-1} rate window. E (0.09) is scaled down by a factor of a thousand.

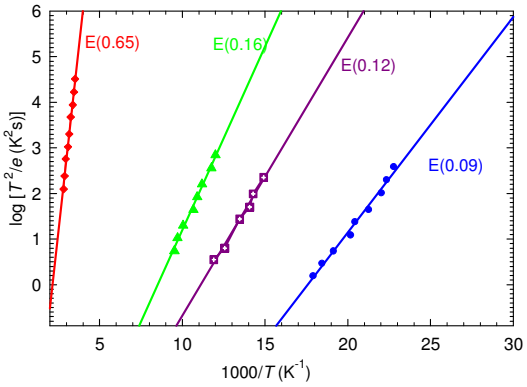

Figure 5 (b). The corresponding Arrhenius plots for the DLTS defects.

Table 2 below summarizes the properties of the detected defects in terms of the activation energies, the peak temperature and the apparent capture cross sections.

Table 2. Activation energies and apparent capture cross sections of identified defects. The spectra were recorded at a rate window of 1000 s^{-1}.

Defect	Activation energy (eV)	Capture cross section (cm^2)	T_{peak} (K)
E(0.09)	0.09	6×10^{-14}	55
E(0.12)	0.12	2×10^{-15}	70
E(0.16)	0.16	2×10^{-15}	110
E(0.65)	0.65	6×10^{-16}	350

The electron beam induced defects, (E_C – 0.160) eV and (E_C – 0.121) eV below the conduction band edge, have average concentrations of 3×10^{11} cm^{-3} and 1×10^{12} cm^{-3} respectively. These two peaks

were not detected in the sample with resistively evaporated Schottky contacts. Also, we only detect these peaks in the 7.1×10^{15} cm^{-3} doped sample and not in the 1.96×10^{16} cm^{-3} doped sample.

4. Conclusion

I-V-T measurements of W/Pd Schottky contacts on n-4H SiC have shown that current transport below 140 K is not *TE* dominated. The anomalous temperature dependencies of n and Φ_{BO}; and, the very small Richardson constant obtained from the conventional the Richardson plot suggests an inhomogeneous MS interface. A modified Richardson constant ($25.5 Acm^{-2}K^{-2}$) was also not close to the expected value (149 $Acm^{-2}K^{-2}$) and a mean Schottky barrier height of 1.7 eV, was obtained from considering the inhomogeneities to be Gaussian distributed. DLTS measurements reveal the existence of two prominent peaks with activation energies of 0.09 eV and 0.67 eV. Two additional peaks with activation energies of 0.12 eV and 0.16 eV which we attribute to the e-beam metallization process and are dopant concentration dependent, are reported in this work.

Acknowledgements

We acknowledge the financial assistance by the South African National Research Foundation and colleague Sergio Coelho for the e-beam metallization.

References

[1] W. Harrell, J. Zhang, K. Poole, J. Electronic Materials, **31** 10 (2002) 1090-1095(6)
[2] S. Chang, S. Wang, K. Uang, B. Lion, Solid-State Electronics 49 (2005) 1937-1941
[3] J. Grant, W. Cunningham, A. Blue, V. O'Shea, J. Vaitkus, E. Gaubas, M. Rahman, Nuclear Instru. & Methods in Phys. Reaserch A546 (2005) 213-217
[4] V. Kazukauskas, J. V. Vaitkus Opto-Electronics Review 12 (4) 377-382
[5] F. Nava, A. Castaldini, A. Cavallini, P. Errani, V. Cindro IEEE Trans. On Nucl. Scie. 538 5 (2006) 2977-2982
[6] F. C. Beyer, C. Hemmingson, H. Pedersen, A. Henry, E. Janzen, J. Isoya, N. Morishita, T. Ohshima J. Appl. Phys. 109 103703 (2011)
[7] A. Castaldini, A. Cavallini, L. Rigutti, F. Nava, S. Ferrero, F. Giorgis, J. Appl. Phys. 98 0503706 (2005)
[8] P. B. Klein, B. V. Shanabrook, S. W. Huh, A.Y. Polyakov, M. Skowronski, J. J. Sumakeris, M. J. Oloughlin, Appl. Phys. Lett. 88 052110 (2006)
[9] S. M. Sze, Physics of Semiconductor devices, 2nd Edn. John Wiley and sons, New York, 1981
[10] E. H. Rhoderick, R. H. Williams, Metal – Semiconductor Contacts, Claredon Press, Oxford University Press, Oxford 1988 19
[11] M. K. Hudait, S. B. Krupanidhi, Physica B 307 (2001) 125-137
[12] S. K Noh, K. N. Jeon, S. E. Park, S. I. Ban, C. R. Lee, S. J. Son, K. Y. Lim, H. J. Lee (1999) *Sae MulliSae Mulli* 39 (4) p. 271-276
[13] T. Tung, Phys. Rev. B 45 (1992) 13509
[14] R. F. Schimitsdorf, T. U. Kampen, W. Monch, Surf. Sci. 324 (1995) 249
[15] B. Abay, G. Cankaya, H. S. Guder, H. Efeoglu and Y. K. Yogurtcu, J. Semicond. Sci. Technol.18 (2003) 75-81
[16] J. H. Werner, H. H. Guttler. J. Appl. Phys 69 (1991) 1522